



Pharmaceutics, Drug Delivery and Pharmaceutical Technology

## New Delivery Route of Gambogic Acid Via Skin for Topical Targeted Therapy of Cutaneous Melanoma and Reduction of Systemic Toxicity



Ding Zhang<sup>a</sup>, Wei Wang<sup>a</sup>, Tao Hou<sup>b</sup>, Yanjun Pang<sup>c</sup>, Chao Wang<sup>c</sup>, Shuai Wu<sup>a</sup>, Qing Wang<sup>a,\*</sup>

<sup>a</sup> State Key Laboratory of Fine Chemicals, Department of Pharmaceutical Sciences, School of Chemical Engineering, Dalian University of Technology, Dalian, Liaoning 116024, China

<sup>b</sup> Key Laboratory of Separation Science for Analytical Chemistry, Dalian Institute of Chemical Physics, Chinese Academy of Sciences, Dalian, Liaoning 116023, China

<sup>c</sup> Liaoning Institute for Drug Control, Shenyang, Liaoning 110036, China

### ARTICLE INFO

#### Article history:

Received 1 September 2020

Revised 21 December 2020

Accepted 21 December 2020

Available online 26 December 2020

#### Keywords:

Gambogic acid  
Melanoma  
Topical delivery  
Penetration  
Accumulation  
Azone  
Propylene glycol  
Systemic toxicity

### ABSTRACT

Cutaneous melanoma is the deadliest form of skin cancer, and gambogic acid (GA) exhibits potent anti-melanoma activity. However, clinical application of GA via intravenous injection and oral administration is limited by systemic toxicity and rapid metabolism in the blood. Here, we developed a new, topical route of GA delivery for anti-melanoma activity and reduction of systemic toxicity. The results indicated that the barrier of the stratum corneum (SC) and low diffusion of GA in the hydrophilic viable skin (epidermis and dermis) limited the GA penetration through intact skin. The combination of azone (AZ) and propylene glycol (PG) showed obvious synergistic effects on skin penetration by GA via improving the permeability of the SC and greatly increasing the skin accumulation of GA, thereby forming a high drug concentration in the skin and achieving a topical targeted treatment of melanoma. In addition, GA (AZ–PG) achieved the same anti-melanoma effect via topical delivery as via intravenous injection. Intravenous injection and oral administration of GA induced remarkable pathological changes in various organs in mice, whereas GA was not toxic to various organs or to the skin via topical delivery. These findings indicated that topical administration of GA is an alternative route for melanoma treatment.

© 2021 Published by Elsevier Inc. on behalf of the American Pharmacists Association.

### Introduction

Malignant melanoma is a highly malignant tumor arising from melanocytes, and it occurs in the skin, eyeballs, digestive tract, reproductive system and other parts.<sup>1</sup> Cutaneous melanoma, located in the basal lamina of epidermis, is the most deadly form among skin cancers due to its high malignancy and early metastasis.<sup>2–4</sup> The morbidity and mortality of melanoma are the highest among people aged from 25 to 29, with an average survival time of only 6–9 months after metastasis.<sup>5</sup> In recent years, melanoma has become one of the fastest growing tumors, and the annual growth rate of the disease is 3–5%, approximately 132,000 newly diagnosed cases and 48,000 deaths worldwide every year.<sup>6,7</sup> In particular, the incidence and mortality of melanoma in China are

significantly higher than the global average.<sup>8</sup> At present, surgical resection, chemotherapy, radiotherapy, targeted therapy and immunotherapy are applied in the clinical treatment of melanoma.<sup>9–11</sup> Despite recent advances in the targeted therapy and immunotherapy, chemotherapy is still one commonly used therapeutic method as most anti-tumor drugs directly aim at and kill tumor cells with a significant and lasting effect on tumor.<sup>12,13</sup>

Gambogic acid (GA) is a major effective ingredient derived from gamboge resin and has been confirmed to be effective against a wide range of cancers, such as gastric cancer, breast cancer, liver cancer, lung cancer, colon cancer, skin cancer, etc.<sup>14–19</sup> Multiple anticancer mechanisms are involved, including cell cycle arrest, induction of apoptosis, telomerase inhibition, anti-angiogenesis and anti-metastasis.<sup>19–23</sup> Being a broad-spectrum anticancer active component, GA brings a prospect in the prevention and treatment of cancer with advantage of being multi-target.<sup>24</sup> GA has been reported to be toxic to B16–F10 cells and possess significant inhibitory effect on melanoma-bearing mice.<sup>25,26</sup>

\* Corresponding author.

E-mail address: [qwang@dlut.edu.cn](mailto:qwang@dlut.edu.cn) (Q. Wang).

However, due to the extremely short half-life of GA in plasma,<sup>27,28</sup> multiple injections of GA into patients is necessary to meet the treatment requirements of malignant tumors, and which leads to side effects, such as pain, phlebitis, liver damage, heart toxicity, etc.<sup>29</sup> In view of the aforementioned shortcomings, the evaluation of clinical superiority of GA via intravenous injection in the treatment of tumors is failed in Phase III of the clinical trial. In addition, GA is poorly absorbed *in vivo* via oral administration and its area under curve (AUC) value is very low ( $24.3 \pm 6.96$  ng/h.mL) in rats,<sup>30</sup> moreover, GA administered orally also shows high toxicity to various organs of rats.<sup>31</sup> Therefore, clinical application of GA via intravenous injection and oral administration is limited. To address these issues, on account of the low absorption of GA by oral administration, a number of research have been carried out on improving the bioavailability and efficacy of GA through intravenous injection by liposomes, micelles and nanoparticles, at the same time avoiding its stimulation on blood vessels and organs *in vivo*.<sup>25,27,32–34</sup> However, corresponding preparations were still limited by drug instability, low drug loading, complex preparation process and low reproducibility, resulting in difficulties of production from laboratory to industrial scale.<sup>35,36</sup> Besides, these excipients may also be difficult to degrade and possess systemic toxicity *in vivo*. Up to now, no related intravenous or oral preparations of GA have been clinically and commercially available. It is therefore necessary to find a new delivery route of GA with reduced toxicity and maintained efficiency, serving as a breakthrough in the melanoma treatment.

Topical drug delivery (TDD) is a treatment approach in which a medication is directly delivered to the disease site of skin at a high local concentration so as to avoid the drug from entering the blood circulation, thus achieving a high efficacy at a small delivery area. Compared with intravenous injection and oral administration, TDD exhibits great advantages in protecting the drug from the first pass effect in liver and from the damage in gastrointestinal tract caused by enzymes, digestive juices, pH, etc., as well as showing low systemic toxicity, few side effects, convenience for use and good patient compliance.<sup>37–39</sup> Using TDD as an effective treatment for cutaneous melanoma, Jiang et al. developed a paclitaxel transdermal gel for topical melanoma treatment.<sup>40</sup> Labala et al. reported to deliver imatinib mesylate by topical application using layer-by-layer polymer-coated gold nanoparticles against the melanoma.<sup>39</sup> To date most of the studies on GA in the melanoma treatment focus on the intravenous injection route, few on the skin administration. This study, investigated the skin permeability, anti-melanoma activity and safety of GA through topical delivery, and evaluated the feasibility of its anti-melanoma activity.

## Materials and Methods

### Materials

GA (purity  $\geq 98\%$ ) was obtained from Chengdu Rui Sifen Bio-Tech Co., Ltd (Chengdu, China). Azone (AZ) was purchased from Shanghai Aladdin Bio-Tech Co., Ltd (Shanghai, China). Propylene glycol (PG), 1-methyl-2-pyrrolidone (NMP), isopropyl myristate (IPM), polyethylene glycol-400 (PEG-400) and tween-80 were purchased from Sinopharm Chemical Reagent Co., Ltd (Shanghai, China). Carbopol 974P was purchased from Beijing Guoren Yikang Tech Co., Ltd (Beijing, China). Acetonitrile and methanol (HPLC grade) were purchased from Mreda Technology Co., Ltd (Beijing, China). All other chemicals and solvents were of analytical grade.

### Cell Culture

B16–F10 cells were obtained from the Cell Bank of Chinese Academy of Sciences (Shanghai, China). The cells were cultured in

RPMI-1640 medium (Thermo Fisher Scientific, Waltham, MA, USA) supplemented with 10% FBS (Thermo Fisher Scientific, Waltham, MA, USA) and maintained at 37 °C in a humidified atmosphere containing 5% CO<sub>2</sub>.

### Animals

Male C57BL/6J mice ( $20 \pm 2$  g) and male BALB/c nude mice ( $20 \pm 2$  g) were provided by Liaoning Changsheng Bio-Tech Co. Ltd (Benxi, China). SD rats ( $200 \pm 20$  g) and male KM mice ( $20 \pm 2$  g) were purchased from Dalian Medical University (Dalian, China). Animals were housed with free access to standard food pellet and water in plastic cages at a controlled temperature of 20–22 °C and adapted to a 12 h light–12 h dark cycle. All animal experiments were conducted in accordance with EU Directive 2010/63/EU for animal experiments and the Biology and Medical Ethics Committee of Dalian University of Technology (Dalian, China). All efforts were made to minimize the animals suffering and to reduce the number of animals used.

### Analysis of GA

GA was analyzed by a high performance liquid chromatography (HPLC) equipped with a UV detector (Shimadzu, Kyoto, Japan). Separation was achieved with a diamosil C18 (2) column ( $150 \times 4.6$  mm; particle size 5  $\mu$ m) (Dikma Tech, Beijing, China) maintained at 30 °C. A mobile phase consisted of 90% organic phase (a mixture of acetonitrile and methanol (1:1)) and 10% water phase (containing 0.1% phosphoric acid) was kept at a flow rate of 1.0 mL/min and monitored at a wavelength of 360 nm. The standard curve was developed using linear regression analysis in the range of 0.078–10  $\mu$ g/mL ( $R^2 = 0.9999$ ). The relative standard deviations of inter- and intra-day precision were below 1.0%, and the recovery of GA by ultrasonic extraction was between 95 and 105%.

### Melting Point Measurement

The melting point of GA was investigated by a differential scanning calorimetry (DSC, Shimadzu, Japan). GA and Al<sub>2</sub>O<sub>3</sub> samples of the same weight were placed in aluminum pans separately. DSC measurements were carried out at a temperature range of 25–200 °C and a nitrogen flow of 50 mL/min. The heating rate was 10 °C per minute. All samples were prepared in triplicate.

### Apparent Solubility Determination

The apparent solubility of GA was determined by a shake-flask method. An excess amount of GA was added into 5.0 mL of deionized water, and the flask was shaken at  $25 \pm 0.5$  °C for 24 h. Next, the solution was centrifuged at 10,000 rpm for 10 min and the supernatant was filtered by a 0.45  $\mu$ m membrane. Then the concentration of GA was determined by the HPLC method. All samples were analyzed in triplicate.

### Apparent Partition Coefficient Determination

Water and *n*-octanol (mixed with a ratio of 1:1) were pre-saturated at  $25 \pm 0.5$  °C for 24 h, and then the oil phase and water phase were separated by centrifugation at 10,000 rpm for 10 min. A certain amount of GA was dissolved in the water phase (*n*-octanol saturation) by ultrasound for 30 min, and then 8.0 mL water phase and 1.0 mL oil phase were mixed and shaken at  $25 \pm 0.5$  °C for 24 h. After that, the solutions were centrifuged at 10,000 rpm for 10 min. The concentrations of GA in oil phase and water phase were analyzed by the HPLC method, and the apparent partition

coefficient of GA described as  $\log P$  was calculated by the formula:  $\log P = \log (C_o/C_w)$ , in which  $C_o$  and  $C_w$  represent concentrations of GA in oil phase and water phase, respectively. All samples were analyzed in triplicate.

#### *In Vitro Penetration of GA in Intact Skin and Stripped Skin*

The purpose of this experiment was to investigate the effect of the stratum corneum (SC) on permeability for GA *in vitro*. Saturated GA was used as a donor solution. To ensure that the saturated GA in the donor chamber was stirred throughout the experiment and to avoid the issue of undissolved GA solid in the saturated solution adsorbing on the skin surface and interfering with skin penetration, the penetration of GA was evaluated using a horizontal (side-by-side) diffusion cell system (KX-5HPC, Dalian Kexiang Technology Co., Ltd., Dalian, China) with an effective diffusion area of 0.79 cm<sup>2</sup> and a 5.0 mL receptor chamber in intact skin and in stripped skin. Male nude mice were sacrificed by cervical dislocation. Next, dorsal skin was cut with subcutaneous fat removed to prepare the intact skin. The SC of the intact skin was removed 15–20 times by tape stripping to prepare stripped skin. The thickness of the prepared skin was measured using a vernier caliper. The skin was mounted between the donor and receptor chambers with the SC facing the right-hand side chamber. The left-hand side chamber (receptor compartment) was filled with a phosphate buffer saline (PBS) medium (pH 5.5, containing 0.5% tween-80), whereas the right-hand side chamber (donor compartment) was filled with a saturated solution of GA (896.91 ± 109.19 µg/mL) in a PBS medium (pH 5.5, containing 0.5% tween-80) to maintain a constant source of drug. In addition, the diffusion cell was kept at 32 ± 0.2 °C by electric heating, and both the donor and receptor compartments were under agitation by a magnetic stirrer at 600 rpm throughout the experiment. Next, 0.3 mL of samples was taken from the receptor compartment at various time points (0, 3, 6, 9, 12, 15, 18, 21, 24, and 27 h), and replaced by fresh medium of the same volume. Finally, the GA concentrations in the solutions were determined by the HPLC method. All experiments were sampled and analyzed from four individual skin membranes. Related permeation parameters were calculated according to the following equations:

$$Q_t = \frac{C_n \times V + \sum C_{n-1} \times V_n}{A} \quad (1)$$

$$P_m = \frac{J_{ss}}{C} \quad (2)$$

where  $Q_t$  is cumulative amount of GA permeated per unit area of skin (µg/cm<sup>2</sup>),  $C_n$  is a concentration of GA determined at No. n sampling interval (µg/mL),  $C_{n-1}$  is a concentration of GA determined at No. n-1 sampling interval (µg/mL),  $V$  is the volume of individual diffusion cell (5.0 mL),  $V_n$  is the volume of sampling aliquot (0.3 mL), and  $A$  is effective diffusion surface area (0.79 cm<sup>2</sup>).  $P_m$  is permeation coefficient (cm/h), and  $C$  is the initial concentration of GA in the donor compartment.

#### *In Vitro Effect of pH on the Penetration of GA Through Intact Skin*

To investigate the effect of pH on the permeation of GA *in vitro*, a vertical diffusion cell system (KX-10VPC, Dalian Kexiang Technology Co., Ltd., Dalian, China) with an effective diffusion area of 1.77 cm<sup>2</sup> and a 10.0 mL receptor compartment was used, similar to the use state of transdermal absorption preparation. Dorsal skin of the same thickness from male normal mice was mounted between the donor and receptor chambers with the SC facing the donor chamber. The receptor chamber was filled with a PBS medium (pH

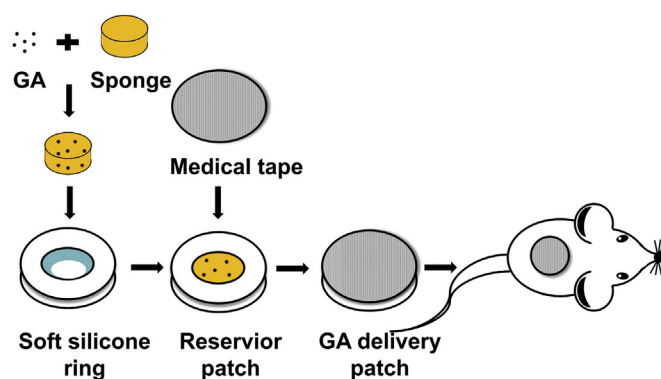


**Fig. 1.** Schematic illustration of preparation and application of GA as a patch for topical delivery.

5.5, containing 0.5% tween-80), and the donor chambers were individually filled with 0.5 mL of various GA formulations dissolved in 0.5% tween-80 aqueous solutions (pH 5.5, 6.5, 7.5, and 8.5, 500 µg/mL of GA). The diffusion cell was maintained at 32 ± 0.2 °C with a magnetic stirrer of 600 rpm. Next, 0.5 mL of the medium was sampled from the receptor chamber after 12 h or 24 h and concentrations of GA were determined by the HPLC method. To evaluate the skin accumulation of GA, residual GA was removed from the skin surface by ethanol and water at the end of the experiment, and then the skin was cut into small pieces and placed in 1.0 mL of acetonitrile. GA was extracted from the skin by an ultrasound system (SK5200LHC, Shanghai, China) at room temperature (25 ± 0.5 °C) for 60 min. Next, these samples were filtered (0.45 µm) and the GA concentration in the skin was determined by the HPLC method. All experiments were based on four individual skin membranes.

#### *In Vitro Effect of Chemical Enhancers on the Penetration of GA Through Intact Skin*

The effect of chemical enhancers on the GA penetration through the dorsal skin was investigated by a vertical diffusion cell system as described above. The procedure for preparation of various GA formulations was as follows: 50 mg of GA was dissolved in tween-80 to prepare 100 mg/mL GA solution beforehand, and then 0.1 mL of GA solution (100 mg/mL) and various amounts of enhancers (AZ, PG, NMP, or IPM) were added to deionized water to prepare 500 µg/mL GA aqueous solution. Then, 10.0 mL of PBS (pH 5.5, containing 0.5% tween-80) and 0.5 mL of various GA formulations (AZ, PG, NMP, or IPM, 500 µg/mL of GA, containing 0.5% tween-80) were added to the receptor and donor compartments, respectively. The diffusion cell was continuously stirred at 600 rpm and kept at 32 ± 0.2 °C. After 24 h, the concentrations of GA in the receptor chamber and skin were determined as described above. All experiments were based on four individual skin membranes.

#### *In Vivo Penetration Study*

Male C57BL/6J mice were divided into a control group (four mice, no enhancer, containing 0.5% tween-80, 800 µg/mL of GA aqueous solution) and an enhancer group (four mice, containing 0.5%AZ, 1% PG, and 0.5% tween-80, 800 µg/mL of GA aqueous solution). Hair on the dorsal skin in an area of about 3 × 3 cm<sup>2</sup> was removed with a razor, and 48 h were allowed to pass for full recovery of the skin. For *in vivo* experiments, we designed a delivery patch consisting of a non-irritating strong adhesive silicone ring (diameter: 15 mm, height: 4 mm; 3 M company, St. Paul, MN, USA)

**Table 1**  
The Physical Properties of GA (n = 3, Mean ± SD).

	Molecular Weight (g/mol)	Melting Point (°C)	Apparent Solubility (µg/mL, 25 ± 0.5 °C)	Log P (25 ± 0.5 °C)
GA	628.75	69.90–70.72	0.56 ± 0.07	4.32 ± 0.11

and a non-absorbent medical tape (Shanghai Xisen Material Technology Co., Ltd. Shanghai, China) as presented in Fig. 1. A porous round sponge soaked with 0.5 mL of GA aqueous solution (with or without enhancer) was placed in the silicone ring and the top layer of patch was fixed with a medical tape to form a closed delivery system. Then, the delivery patch was attached to the mice skin for 6 h to ensure that GA had sufficient contact with the skin. After the experiments, the mice were sacrificed and residual GA was removed from the skin surface by ethanol and water. The test skin was then removed with a scalpel and cut into small pieces. The GA extraction method was as described above. GA concentrations in the skin were analyzed by the HPLC method.

#### In Vivo Antitumor Effect Study

Next, 60 µL of RPMI-1640 containing B16–F10 cells (the cell density:  $3.3 \times 10^5$  cells/mL) was injected intradermally into each C57BL/6J male mouse, and the animals were individually housed. Once the tumor diameter reached 2–3 mm (in approximately two weeks), 36 mice were randomized into six groups (six mice per group), and three routes of administration were adopted. The mice were treated in the following regimens: (1) blank group: without any treatment; (2) AZ–PG topical delivery group: 0.5 mL aqueous solution (without GA, containing 0.5% AZ, 1% PG, and 0.5% tween-80) smeared on the tumors for 6 h every day (as in Fig. 1); (3) GA + AZ–PG topical delivery group: 0.5 mL GA aqueous solution (containing 0.5%AZ, 1% PG, and 0.5% tween-80, 800 µg/mL of GA) smeared for 6 h every day (as in Fig. 1); (4) GA topical delivery group: 0.5 mL GA aqueous solution (without enhancer, containing 0.5% tween-80, 800 µg/mL of GA) smeared for 6 h every day (as in Fig. 1); (5) GA intravenous injection group: injection of GA (4 mg/kg) every other day in the tail vein; and (6) GA oral administration group: intragastric administration of GA (20 mg/kg) every other day. The tumor volume (according to the formula<sup>27</sup>: volume =  $0.52 \times \text{length} \times \text{width}^2$ ) and the body weight of each mouse were measured daily. Because the skin would rupture after 11 days of topical delivery due to the excessive tumor growth, we stopped administration of GA on day 10 in order to accurately

evaluate the anti-melanoma activity of GA through the intact skin. Mice were euthanatized after treatments, after which the tissues (including heart, liver, spleen, lung, kidney, and tumor) were collected and weighed. The tissue sections were stained by the hematoxylin-eosin staining (H&E). The stained tissue sections were visualized under microscope (Olympus CX43).

#### Skin Irritation Study

The skin irritation caused by GA was evaluated according to the organization for economic co-operation and development (OECD) guidelines with little modification.<sup>41</sup> Eighteen SD rats ( $200 \pm 2$  g; nine male and nine female) were selected to the test for convenient operation due to its small size, and the skin irritation of these animals of each sex to GA could be fully investigated. Rats were divided randomly into three groups (six animals per group). In each rat, hair on both sides of the dorsal skin at an area of about 10 cm<sup>2</sup> was removed by a razor 24 h before the day of the experiment. Rats with undamaged skin were marked as the intact skin group. The stripped skin group included rats in which SC was removed 20 times by tape peeling prior to the first administration. The scratched skin group included rats that were punctured in “#” pattern by a sterile needle until their skin bled.

Next, 0.5 g of GA gel (containing 0.8% carbopol 974P and 0.5% tween-80 as vehicle, 800 µg/mL of GA) was smeared on the right-side dorsal skin for 6 h daily, while on the left side, an equivalent amount of vehicle was applied as negative control. The rats were wrapped with sterile gauze and adhesive tape to avoid movement. In each rat, the skin was observed every day after residual sample was removed for 1 h. After the last administration, skin irritation was continuously examined at 24, 48, and 72 h, or at additional time points. A numerical scoring system was used to rate skin reactions on a scale from 0 to 4, ranging from no signs to severe signs (Table S1, supplementary material). In addition, the skin was cut off and investigated after H&E staining. The stained tissue sections were visualized under a microscope (Olympus CX43).

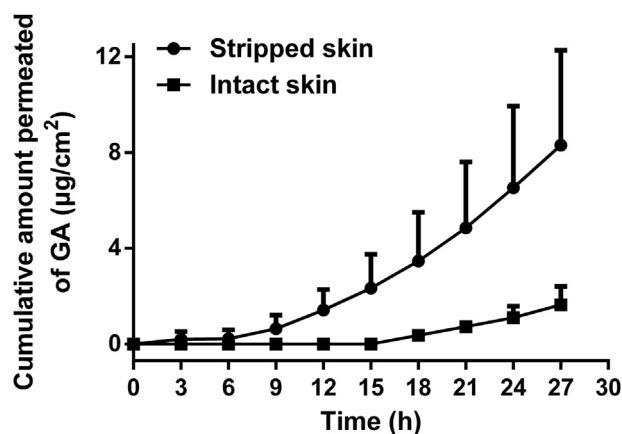


**Fig. 2.** Permeated amount versus time profiles of GA through intact skin and stripped skin for 27 h *in vitro* (n = 4).

#### Statistical Analysis

Statistical analysis of all samples was carried out with SPSS 21.0, and values were presented as means ± standard deviation of at least three independent determinations. *p* values were obtained using two-tailed unpaired Student's *t* tests. Results were determined to be statistically significant as *p* < 0.05.

**Table 2**  
Permeation Parameters of GA Through Intact Skin and Stripped Skin at 27 h *In Vitro* (n = 4, Mean ± SD).

Permeation Parameters	Intact Skin	Stripped Skin
$Q_{27}$ (µg/cm <sup>2</sup> )	1.63 ± 0.77	8.31 ± 3.96
$J_{ss}$ (µg/cm <sup>2</sup> /h)	0.14 ± 0.06	0.50 ± 0.22
$t_d$ (h)	15.81 ± 0.68	11.11 ± 1.14
$P_m$ (cm/h)	$(1.57 \pm 0.70) \times 10^{-4}$	$(5.58 \pm 2.40) \times 10^{-4}$

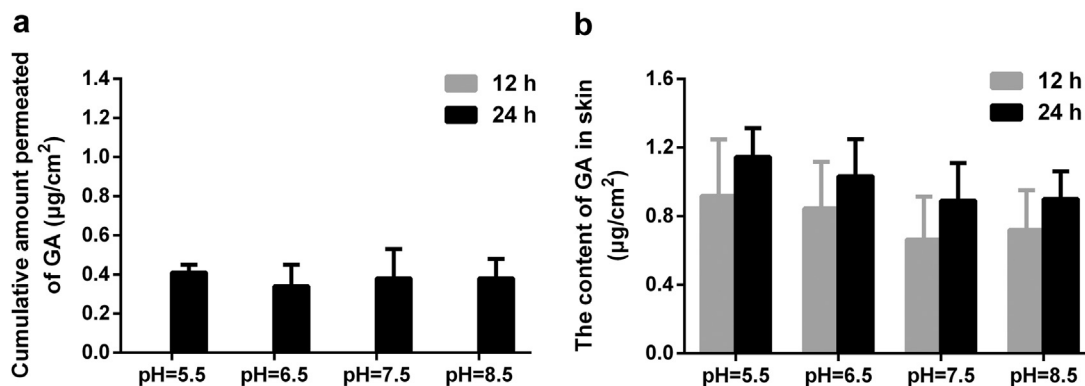


**Fig. 3.** Effect of pH on the penetration of GA through intact skin *in vitro* ( $n = 4$ ). (a) Cumulative amount permeated of GA at 12 h and 24 h; (b) the content of GA in skin at 12 h and 24 h.

## Results

### Physical Properties of GA

The melting point of GA was low at a range of 69.90–70.72 °C (Table 1), and GA exhibited poor aqueous solubility ( $0.56 \pm 0.07 \mu\text{g}/\text{mL}$ ). In addition, the log  $P$  value ( $4.32 \pm 0.11$ ) showed that GA had strong lipophilicity.

### In Vitro Penetration of GA Through the Intact Skin and Stripped Skin

The diffusion cell system was employed to evaluate the GA penetration through the intact skin and stripped skin of nude mice *in vitro*. GA was detected in the receptor solution of the stripped skin group at 9 h, while it was detectable in the solution of the

intact skin group after 15 h (Fig. 2). In addition, the steady-state flux ( $0.50 \pm 0.22 \mu\text{g}/\text{cm}^2/\text{h}$ ) and cumulative penetration amount ( $8.31 \pm 3.96 \mu\text{g}/\text{cm}^2$ ) of GA at 27 h in the stripped skin were significantly higher than in the intact skin group ( $0.14 \pm 0.06 \mu\text{g}/\text{cm}^2/\text{h}$  and  $1.63 \pm 0.77 \mu\text{g}/\text{cm}^2$ , respectively) (Table 2). The lag time of GA in the stripped skin was 11.11 h, which was shorter than in the intact skin (15.81 h) (Table 2), but it still took a relatively long time for GA to reach a steady penetration state. The permeation coefficient of GA in the stripped skin was three times higher than that in the intact skin.

### In Vitro Effect of pH on the Penetration of GA Through the Intact Skin

A series of GA formulations at different pH values (5.5, 6.5, 7.5, and 8.5) were prepared to investigate the effect of pH on the

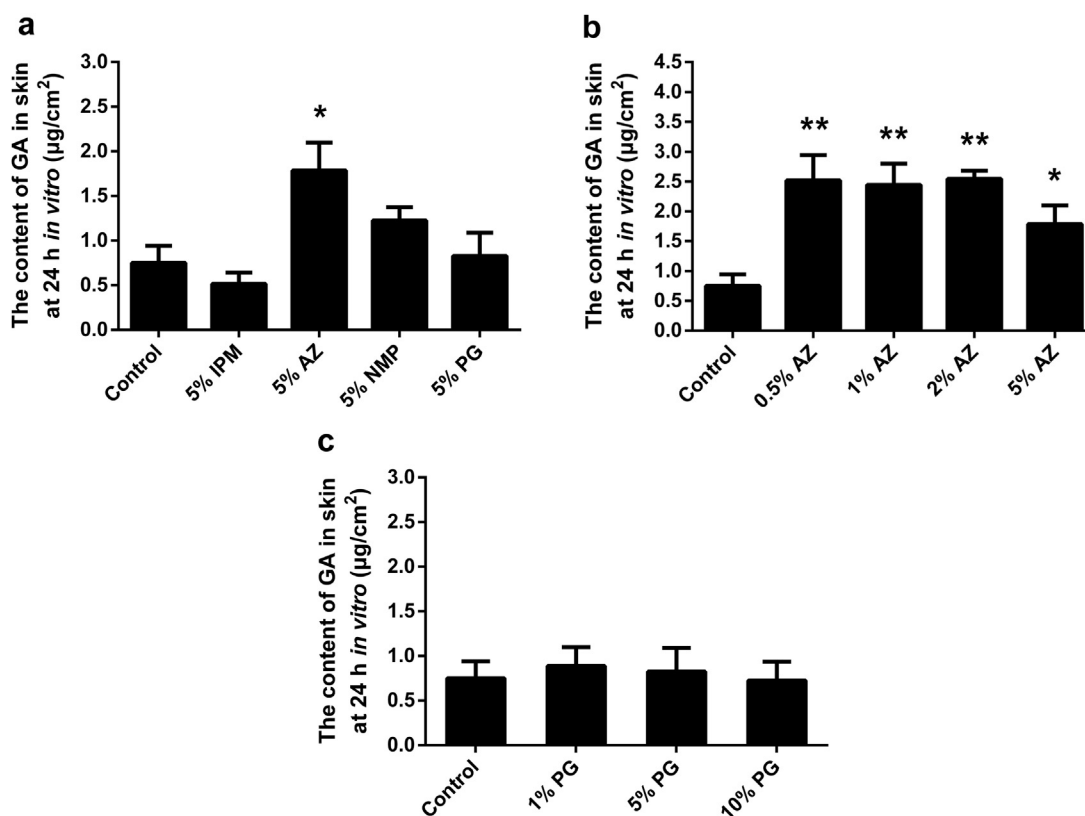


**Fig. 4.** Effect of chemical enhancers on the accumulation of GA in the intact skin at 24 h *in vitro* ( $n = 4$ ): (a) Types of chemical enhancers; \* $p < 0.05$ , \*\* $p < 0.01$  vs control; (b) different concentrations of AZ; \* $p < 0.05$ , \*\* $p < 0.01$  vs control; (c) different concentrations of PG.

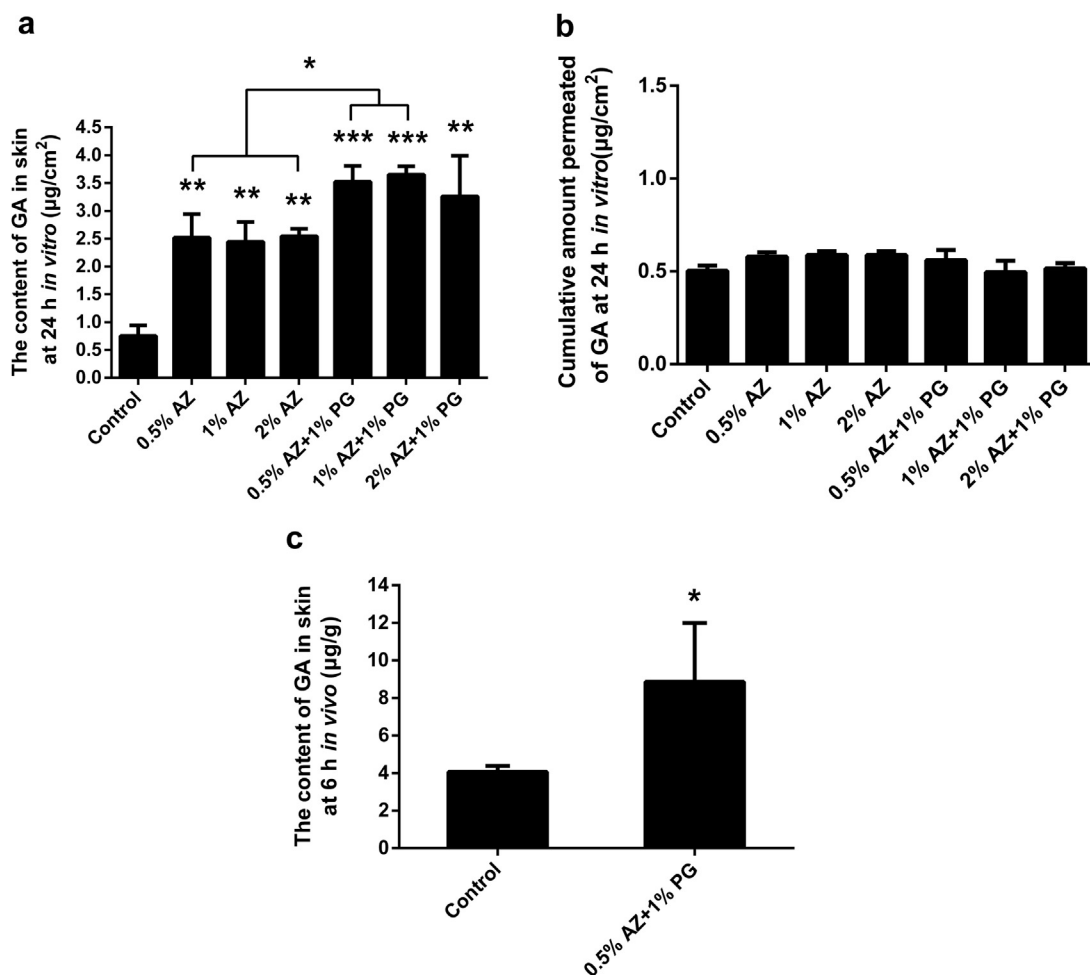


**Fig. 5.** Effect of chemical enhancers on the penetration of GA *in vitro* and *in vivo* (n = 4): (a) Effect of AZ and AZ–PG on the skin accumulation of GA at 24 h *in vitro*; \* $p < 0.05$ , \*\* $p < 0.01$ , \*\*\* $p < 0.001$  vs control; \* $p < 0.05$  vs AZ alone; (b) Effect of AZ and AZ–PG on the cumulative amount permeated of GA at 24 h *in vitro* (n = 4); and (c) Effect of AZ–PG on the accumulation of GA in the dorsal skin of male mice at 6 h *in vivo* (n = 4); \* $p < 0.05$  vs control.

penetration of GA *in vitro*. For all formulations, no GA was detected in the receptor solution at 12 h, but GA was detected at 24 h with no significant difference in its cumulative penetration amount between different pH formulations ( $p > 0.05$ , Fig. 3a). Additionally, a slight downward trend of GA content in the skin was observed at both 12 h and 24 h when the pH of formulations increased from 5.5 to 8.5, but there was no significant difference observed between the formulations ( $p > 0.05$ , Fig. 3b). Briefly, the penetration of GA during 24 h *in vitro* was not significantly affected by pH in the range from 5.5 to 8.5.

#### *In Vitro* Effect of Chemical Enhancers on the Penetration of GA Through the Intact Skin

Chemical enhancers were used to improve the penetration of GA through the intact skin. Since only a small portion of the total GA content penetrated through the intact skin at 24 h, we investigated the effect of enhancers on the skin accumulation of GA. The results showed that compared with the control group, the GA content increased by 2.38 times ( $p < 0.05$ ) and 1.64 times when the skin was treated by AZ and NMP, respectively (Fig. 4a). In contrast, the GA content did not increase after treatment by PG or IPM. The effect of AZ concentration was subsequently studied because AZ obviously enhanced the GA accumulation. In comparison with the control group, the GA skin content was significantly increased by 0.5%–5%

AZ ( $p < 0.05$ , Fig. 4b). The increase level remained the same when AZ concentrations were between 0.5% and 2%, relatively higher than that in 5% AZ ( $p < 0.05$ ).

Considering the previous reports of obvious synergistic effects of the AZ–PG combination,<sup>42–44</sup> we further investigated the skin penetration by GA after applying the combination of AZ and PG *in vitro*. The GA content in the skin did not change when the skin was treated with PG alone in the concentration range of 1–10% ( $p > 0.05$ , Fig. 4c). However, when 1% PG was added to 0.5%, 1%, and 2% AZ, the GA content notably increased by 4.70, 4.87, and 4.35 times, respectively, compared with the control group ( $p < 0.01$ , Fig. 5a). Moreover, the data from the AZ–PG combination and AZ alone indicated that the addition of PG improved the GA content in the skin for every concentration of AZ (Fig. 5a), suggesting the synergistic effects of AZ–PG on the skin accumulation of GA. In addition, the combination of AZ and PG showed an insignificant effect on the GA cumulative amount permeated at 24 h (Fig. 5b), but it could greatly increase the accumulation of GA in each layer of the skin (Fig. S1, supplementary material). Based on these results, the combination of 0.5% AZ and 1% PG was selected for *in vivo* studies.

#### *In Vivo* Penetration Study

The GA penetration experiments *in vivo* were carried out on the dorsal skin of C57BL/6J mice. After delivery of GA by topical

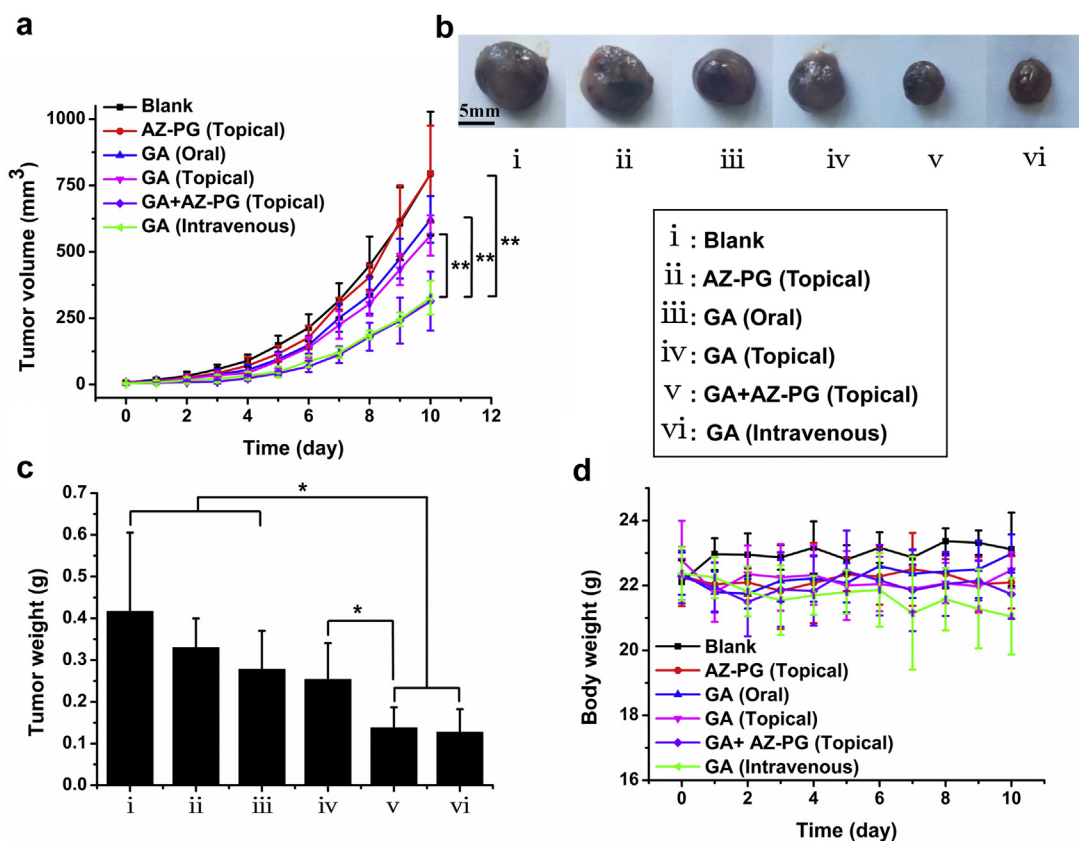


**Fig. 6.** *In vivo* antitumor evaluation of GA delivered via different routes of administration ( $n = 6$ ). (a) Tumor volumes of the B16–F10 melanoma-bearing mice over time;  $**p < 0.01$ ; (b) tumors isolated after 10 days (Scale bar = 5 mm); (c) tumor weights after 10 days;  $*p < 0.05$ ; and (d) body weights of the mice over time.

application for 6 h, the content of GA in the skin without treatment by enhancers was  $4.06 \pm 0.33 \mu\text{g/g}$  (Fig. 5c). However, it increased two-fold to  $8.86 \pm 3.15 \mu\text{g/g}$  after addition of 0.5% AZ and 1% PG ( $p < 0.05$ ), indicating that the combination of 0.5% AZ and 1% PG achieved an obvious synergistic effect on the skin accumulation of GA *in vivo*.

#### *In Vivo* Antitumor Effect Study

The anticancer efficacy of GA via topical delivery, intravenous injection, and oral administration was evaluated in the B16–F10 melanoma-bearing mice. Compared with the blank group and the AZ–PG topical delivery group, growth of tumor volume was slowed down after giving GA for 10 days through oral, topical, and intravenous administrations (Fig. 6a). However, the antitumor efficacy of GA was notably stronger after topical delivery (containing AZ–PG) or intravenous injection compared with oral administration in terms of tumor volume, size and weight ( $p < 0.01$ ,  $p < 0.05$ , Fig. 6a, b and 6c). Of note, tumor volumes and weights were identical for samples treated through intravenous injection and topical delivery (containing AZ–PG) of GA for 10 days ( $p > 0.05$ ,

Fig. 6a and c). The *in vivo* antitumor effect study further demonstrated that the combined use of AZ and PG had a significant effect on the permeation of GA (Fig. 6). In addition, a noticeable decrease in body weight was observed in the intravenous injection group (Fig. 6d), but not in the oral administration and topical delivery groups during the 10-day treatment. Histopathological examination of the tumors showed dense tumor tissues and angiogenesis in the blank group and the AZ–PG topical delivery group (Fig. S4a and S4b, supplementary material). However, after GA treatment, loose tumor tissues were clearly observed in the center of samples in the oral, intravenous injection, and topical delivery groups (Fig. S4c, S4d and S4e). In particular, tumor tissue necrosis and cell apoptosis appeared in both the intravenous injection and topical delivery groups (black arrows, Fig. S4d and S4e). This phenomenon was also observed outside the tumor tissue in the topical delivery group (black arrows, Fig. S4f).

To evaluate the safety of GA *in vivo* through oral, intravenous, and topical administration, we investigated the histopathological appearance of major organs (heart, liver, spleen, lungs, and kidney) after the 10-day treatment. Compared with the blank group, oral and intravenous delivery of GA seriously damaged the liver, spleen,

**Table 3**

Effect of Different Administration Routes of GA on the Organ Coefficient of Mice ( $n = 6$ , Mean  $\pm$  SD,  $*p < 0.05$  vs Blank Group).

	Heart	Liver	Spleen	Lung	Kidney
Blank	$0.48 \pm 0.06$	$5.29 \pm 0.64$	$0.31 \pm 0.04$	$0.62 \pm 0.11$	$1.26 \pm 0.12$
AZ–PG (Topical)	$0.55 \pm 0.07$	$5.59 \pm 0.36$	$0.33 \pm 0.05$	$0.70 \pm 0.04$	$1.41 \pm 0.10$
GA + AZ–PG (Topical)	$0.52 \pm 0.06$	$5.49 \pm 0.41$	$0.27 \pm 0.09$	$0.63 \pm 0.09$	$1.42 \pm 0.04$
GA (Intravenous)	$0.52 \pm 0.04$	$5.85 \pm 0.41$	$0.71 \pm 0.28^*$	$0.76 \pm 0.12$	$1.51 \pm 0.12^*$
GA (Oral)	$0.46 \pm 0.05$	$5.72 \pm 0.39$	$0.31 \pm 0.06$	$0.64 \pm 0.04$	$1.35 \pm 0.10$

lungs, and kidneys (Fig. S5, supplementary material). In the liver, lacunar dilatation of hepatic sinuses and nuclear atrophy of hepatocytes were observed. In the spleen, the marginal area of the spleen corpuscle was blurred, and infiltration tissue was observed in the white pulp region. In the lung tissue, a large number of inflammatory cells were observed around the bronchi. The reduced lumen of glomeruli and congestion of proximal and distal renal tubules were also observed. Moreover, after treatment by GA intravenous injection, the heart showed loose myocardial connective tissues and an enlarged myocardial fiber gap, while the oral administration group showed no obvious pathology in the heart samples. In contrast, there were no remarkable pathological changes in the corresponding organs of the mice treated with GA (AZ–PG) via topical delivery. Additionally, intravenous injection of GA resulted in a higher organ coefficient in the spleen and kidney compared with the blank group (Table 3), while the organ coefficients in the groups treated by oral and skin administration appeared minor. These results indicated that the delivery of GA via topical application was safe.

### Skin Irritation of GA

The irritation effects of GA on the intact, stripped, and scratched skin of rats were studied over a time period of 10 days. No noticeable erythema or edema appeared in the intact skin group when GA gel was continuously applied to the dorsal skin for 7 days (Fig. S6a, supplementary material). After the last administration, the skin was under observation for another three days (72 h) and showed no erythema or edema (Table S2, supplementary material). In the stripped skin group, in which SC was removed by tape stripping, erythema and edema appeared after a one-day application of either the GA-containing gel or the vehicle alone (Fig. S6b), and scabs appeared after two days of treatment. During the 10 days, the control and the GA groups showed no apparent difference in the score of erythema and edema ( $p > 0.05$ , Table S3, supplementary material). During the additional three days, no obvious erythema or edema was observed on the stripped skin in both groups. Similar images were obtained for the scratched skin; erythema and scabs started to be seen in both groups on the first day after exposing the epidermis to the external environment by needle puncturing (Fig. S6c). The skin of both groups was scratched again by the needle on day 4 when the scab almost fell off for further investigation of skin irritation. For the control and GA-treated groups, there was no significant difference in the erythema score within the 10 days ( $p > 0.05$ , Table S4, supplementary material) and no remarkable erythema in the continuous observation during the additional three days. Histological examination was performed on the tested skin of all groups. Each rat was euthanized at 72 h after the last administration, and then the test skin was removed and fixed with 10% neutral formalin. No severe lesions were observed in the epidermis and dermis from the intact skin group after the treatment with GA gel (Fig. S6d). The same results were observed in the stripped skin and scratched skin group in which the GA gel had been applied. These results confirmed that GA caused no skin irritation in rats.

### Discussion

The low melting point (70 °C) of GA implies a high solubility in skin lipids, so that a higher transdermal flux is expected,<sup>45</sup> but its high molecular weight (628.75 g/mol) tends to a low percutaneous flux in skin.<sup>46</sup> In addition, GA showed poor aqueous solubility ( $0.56 \pm 0.07 \mu\text{g/mL}$ ) and strong lipophilicity with  $\log P$  of  $4.32 \pm 0.11$ , suggesting that the diffusion of GA in the skin could be hindered by

hydrophilic surrounding of the epidermis.<sup>47</sup> These physical properties imply that it is difficult for GA to penetrate through the skin.

Nude mice were used for the GA penetration of intact skin and stripped skin *in vitro* due to the minimum effect of hair follicles on drug penetration.<sup>48</sup> GA was reported to be more stable in an acidic surrounding,<sup>49</sup> so in this study, PBS with pH 5.5 was selected as the receiving medium. The results demonstrated that the GA penetration through the intact skin was hindered by the SC (Fig. 2), which served as the most critical barrier to transdermal drug delivery.<sup>50</sup> In addition, the diffusion of GA in the skin was hindered by the hydrophilic environment of viable skin, and it still took a long time for GA to penetrate the viable skin (Table 2). The permeation coefficient, a concentration-irrelevant parameter describing the intrinsic ability of a drug to cross the SC barrier,<sup>46</sup> indicated that it was difficult for GA to penetrate the intact skin, as also confirmed by the physical properties mentioned above. Overall, the GA penetration was mainly hindered by the SC and the hydrophilic surroundings of viable skin.

The drug penetration was influenced by pH of the vehicles as well as the skin.<sup>51</sup> In this study, a slight decrease in the skin GA content was observed at 12 h and 24 h as the pH of formulations increased from 5.5 to 8.5 (Fig. 3b). We speculated that GA is a weakly acidic drug, which resulted in an increase of ionized GA in formulations along with the pH value. Therefore, the diffusion rate of GA through the lipophilic SC subsequently decreased, thus reducing the content of GA in the skin. However, there was no significant difference between the formulations ( $p > 0.05$ ). Additionally, no significant binding of GA in SC and viable skin was found (Fig. S2, supplementary material); hence, dermal toxicity that could be caused by the highly bound drug in the skin is avoided.<sup>52</sup> Besides, drugs could be metabolized, although the viability of metabolic enzymes is significantly lower in the skin (approximately 1–10%) than in the liver.<sup>53</sup> We found that the stability of GA in a fresh mouse liver homogenate was poor, and its concentration decreased by 60% after 12 h incubation (Fig. S3, supplementary material). In contrast, the stability of GA in the corresponding blank solvent (0.5% tween-80 aqueous solution) and fresh skin homogenate was better, and the content of GA at 12 h decreased only by 10% and 20%, respectively. These results suggested that the effect of metabolic enzymes on GA was even less in the skin than that in the liver.

Chemical enhancing is an effective approach to increase drug percutaneous absorption by interacting with skin constituents to promote drug flux.<sup>42,44</sup> In this study, AZ provided a considerable enhancement in the skin accumulation of GA in a concentration-dependent manner ranging from 0.5% to 5%. Despite being a widely used penetration enhancer, PG only offered mild enhancement effects on estradiol and 5-fluorouracil,<sup>43</sup> and it had almost no effect on the GA content in the skin in our work. In addition, the AZ–PG combination has been reported to have obvious synergistic effects,<sup>42–44</sup> which was verified in our study. Importantly, the GA cumulative amount permeated did not increase after adding AZ and PG, but a considerable drug accumulation was obtained in the SC and viable skin (Fig. 5b and Fig. S1), thus achieving topical targeted treatment of cutaneous melanoma and reducing systemic toxicity of GA. The enhancement mechanism of AZ and PG has been reported in a large number of literatures.<sup>44,54,55</sup> In this study, we speculated that PG increased the AZ concentration in the SC so as to enhance the effect of AZ on the GA permeation,<sup>42</sup> but this needs further study. Moreover, possibly due to an extremely small amount of GA in the plasma of mice, no GA was detected both in the control group (without enhancer) and enhancer group (containing 0.5% AZ and 1% PG) under our analysis method when it was applied to the dorsal skin for 6 h *in vivo* (not supplied).

Our study demonstrated the GA toxicity to the B16–F10 cells *in vivo* (Fig. 6). Due to the poor absorption of GA after oral administration *in vivo*,<sup>30</sup> a low concentration of GA was achieved in tumor tissues, and its anti-tumor activity was not obvious in our study (Fig. 6a). However, the antitumor efficacy of GA after intravenous injection and topical administration (containing AZ–PG) was significantly stronger. GA avoided the first-pass effect in the liver via intravenous injection, and it directly entered the blood circulation to arrive to the tumor tissue with toxicity to the solid melanoma. Interestingly, topical delivery of GA (AZ–PG) induced noticeable cell apoptosis and tissue necrosis both outside and in the center of tumor tissues (Fig. S4e and S4f). Probably because only a small portion of GA entered the blood circulation via topical delivery and a large portion remained in the skin. GA accumulated in the epidermis could penetrate the tumor tissue from the outside and directly target the melanoma to kill cells on the outside and in the center of the tumor, as a result achieving the same anti-melanoma effect as it did through intravenous injection. However, the specific anti-melanoma mechanism of GA via topical delivery remains unclear and needs further study.

The toxicity of GA for organs and skin *in vivo* was also evaluated. We noticed a remarkable loss of body weight in mice treated by intravenous injection (Fig. 6d). Body weight loss is an indicator of adverse effects of drugs and chemicals,<sup>56</sup> so GA was toxic in this manner to mice through intravenous injection as also demonstrated by previous studies.<sup>25,27</sup> Toxicity of GA was also confirmed by the remarkable pathological changes in the organs (heart, liver, spleen, lungs, and kidney) of mice after GA treatment via intravenous injection (Fig. S5). Orally administered GA also produced toxicity to various organs. In contrast, we recorded no pathological changes in the various organs of mice treated with GA (AZ–PG) by topical delivery, indicating that topical administration of GA was safe for the vital organs *in vivo*. Additionally, skin irritation is an essential component of toxicity screening,<sup>57</sup> and erythema and edema are reactions to skin irritation.<sup>58</sup> Our results demonstrated that there was no noticeable irritation of the intact rat skin treated by GA (Fig. S6a and S6d). SC is a natural barrier of the skin that protects the epidermis and dermis from infections.<sup>50</sup> In this study, on the stripped skin and scratched skin, erythema appeared in both the control group and the GA gel-treated group with no statistical difference in scores (Fig. S6b and S6c, Tables S2 and S3), and they disappeared on the 7th day of administration. After the last administration, no remarkable erythema or edema was observed on the stripped skin and scratched skin treated with the GA gel during the continuous observation for three days. No significant lesions in the epidermis and dermis of the stripped skin and scratched skin were observed after treatment with GA gel (Fig. S6d), demonstrating that GA caused no skin irritation in rats.

## Conclusions

In summary, we developed a new delivery route of GA via the skin, and the feasibility of its anti-melanoma activity was systematically evaluated. GA exhibited a weak transdermal delivery and a strong local accumulation in the skin with the addition of AZ and PG, which allowed a topical targeted therapy for cutaneous melanoma and avoided the systemic toxicity of the drug. In addition, GA (AZ–PG) delivered by topical application exhibited the same anti-tumor effect as GA delivered by intravenous injection, and its toxicity was remarkably lower than that of intravenous or oral administration. Our study demonstrated the anti-melanoma activity of GA via the topical delivery route was effective and safe, which provides an alternative route in anti-melanoma treatment.

## Notes

The authors declare no competing financial interest.

## Acknowledgements

This work was supported by the National Natural Science Foundation of China, China (No. 81872827) and the Dongguan City's Financial Support Plan for Introducing Innovation Team (No. 2018607202009). We acknowledge the Key Laboratory of Separation Science for Analytical Chemistry at Dalian Institute of Chemical Physics for kindly providing analytical instrument and technical support for cell culture.

## Appendix A. Supplementary Data

Supplementary data to this article can be found online at <https://doi.org/10.1016/j.xphs.2020.12.024>.

## References

- Lo JA, Fisher DE. The melanoma revolution: from UV carcinogenesis to a new era in therapeutics. *Science*. 2014;346(6212):945–949.
- Makhlouf A, Hajdu I, Hartimath SV, et al. (111)In-Labeled glycoprotein non-metastatic b (GPNMB) targeted gemini surfactant-based nanoparticles against melanoma: in vitro characterization and in vivo evaluation in melanoma mouse xenograft model. *Mol Pharm*. 2019;16(2):542–551.
- Jemal A, Siegel R, Xu J, Ward E. Cancer statistics, 2010. *CA Cancer J Clin*. 2010;60(5):277–300.
- Shoo BA, Kashani-Sabet M. Melanoma arising in african-, asian-, latino- and native-American populations. *Semin Cutan Med Surg*. 2009;28(2):96–102.
- Najem A, Krayem M, Perdrix A, et al. New drug combination strategies in melanoma: current status and future directions. *Anticancer Res*. 2017;37(11):5941–5953.
- Xin Y, Li Z, Chan MT, Wu WK. Circulating epigenetic biomarkers in melanoma. *Tumour Biol*. 2016;37(2):1487–1492.
- Ferlay J, Soerjomataram I, Dikshit R, et al. Cancer incidence and mortality worldwide: sources, methods and major patterns in GLOBOCAN 2012. *Int J Cancer*. 2015;136(5):E359–E386.
- CSCO MECo. . *Clinical Practice Guidelines in Oncology: Melanoma*. Beijing: People's Medical Publishing House; 2015:20–22.
- Gray-Schopfer V, Wellbrock C, Marais R. Melanoma biology and new targeted therapy. *Nature*. 2007;445(7130):851–857.
- Rigel DS, Carucci JA. Malignant melanoma: prevention, early detection, and treatment in the 21st century. *CA Cancer J Clin*. 2000;50(4):215–236.
- Keller HR, Zhang X, Li L, Schaidler H, Wells JW. Overcoming resistance to targeted therapy with immunotherapy and combination therapy for metastatic melanoma. *Oncotarget*. 2017;8(43):75675–75686.
- Ozawa Y, Kusano K, Owa T, Yokoi A, Asada M, Yoshimatsu K. Therapeutic potential and molecular mechanism of a novel sulfonamide anticancer drug, indisulam (E7070) in combination with CPT-11 for cancer treatment. *Cancer Chemother Pharmacol*. 2012;69(5):1353–1362.
- Dhar S, Kolishetti N, Lippard SJ, Farokhzad OC. Targeted delivery of a cisplatin prodrug for safer and more effective prostate cancer therapy in vivo. *Proc Natl Acad Sci U S A*. 2011;108(5):1850–1855.
- Liang LL, Zhang ZX. Gambogic acid inhibits malignant melanoma cell proliferation through mitochondrial p66(shc)/ROS-p53/Bax-Mediated apoptosis. *Cell Physiol Biochem*. 2016;38(4):1618–1630.
- Li X, Tang X, Su J, Xu G, Zhao L, Qi Q. Involvement of E-cadherin/AMPK/mTOR axis in LKB1-induced sensitivity of non-small cell lung cancer to gambogic acid. *Biochem Pharmacol*. 2019;169:113635.
- Li CL, Lu N, Qi Q, et al. Gambogic acid inhibits tumor cell adhesion by suppressing integrin beta 1 and membrane lipid rafts-associated integrin signaling pathway. *Biochem Pharmacol*. 2011;82(12):1873–1883.
- Wang S, Xu Y, Li C, et al. Gambogic acid sensitizes breast cancer cells to TRAIL-induced apoptosis by promoting the cross-talk of extrinsic and intrinsic apoptotic signalings. *Food Chem Toxicol*. 2018;119:334–341.
- Wang J, Liu W, Zhao Q, et al. Synergistic effect of 5-fluorouracil with gambogic acid on BGC-823 human gastric carcinoma. *Toxicology*. 2009;256(1–2):135–140.
- Park MS, Kim NH, Kang CW, Oh CW, Kim GD. Antimetastatic effects of gambogic acid are mediated via the actin cytoskeleton and NF-B pathways in SK-HEP1 cells. *Drug Dev Res*. 2015;76(3):132–142.
- Yi T, Yi Z, Cho SG, et al. Gambogic acid inhibits angiogenesis and prostate tumor growth by suppressing vascular endothelial growth factor receptor 2 signaling. *Cancer Res*. 2008;68(6):1843–1850.
- Guo QL, Lin SS, You QD, et al. Inhibition of human telomerase reverse transcriptase gene expression by gambogic acid in human hepatoma SMMC-7721 cells. *Life Sci*. 2006;78(11):1238–1245.

22. Yu J, Guo QL, You QD, et al. Gambogic acid-induced G2/M phase cell-cycle arrest via disturbing CDK7-mediated phosphorylation of CDC2/p34 in human gastric carcinoma BGC-823 cells. *Carcinogenesis*. 2007;28(3):632-638.
23. Zhang CH, Liu J, Tao FX, et al. The nuclear export of TR3 mediated gambogic acid-induced apoptosis in cervical cancer cells through mitochondrial dysfunction. *Rsc Advances*. 2019;9(21):11855-11864.
24. Kale VP, Gilhooley PJ, Phadtare S, Nabavizadeh A, Pandey MK. *Role of Gambogic Acid in Chemosensitization of Cancer*. 2018:151-167.
25. Cai L, Qiu N, Xiang M, et al. Improving aqueous solubility and antitumor effects by nanosized gambogic acid-mPEG(2)(0)(0) micelles. *Int J Nanomedicine*. 2014;9:243-255.
26. Zhao J, Qi Q, Yang Y, et al. Inhibition of alpha(4) integrin mediated adhesion was involved in the reduction of B16-F10 melanoma cells lung colonization in C57BL/6 mice treated with Gambogic acid. *Eur J Pharmacol*. 2008;589(1-3):127-131.
27. Tang WL, Tang WH, Szeitz A, Kulkarni J, Cullis P, Li SD. Systemic study of solvent-assisted active loading of gambogic acid into liposomes and its formulation optimization for improved delivery. *Biomaterials*. 2018;166:13-26.
28. Zheng Z, Ou W, Zhang X, Li Y, Li Y. UHPLC-MS method for determination of gambogic acid and application to bioavailability, pharmacokinetics, excretion and tissue distribution in rats. *Biomed Chromatogr*. 2015;29(10):1581-1588.
29. Zhengtao Z, Jinwan W. Phase I human tolerability trial of gambogic acid. *Chinese Journal New Drugs*. 2007;16(1):79-83.
30. Hua X, Liang C, Dong L, Qu X, Zhao T. Simultaneous determination and pharmacokinetic study of gambogic acid and gambogenic acid in rat plasma after oral administration of *Garcinia hanburyi* extracts by LC-MS/MS. *Biomed Chromatogr*. 2015;29(4):545-551.
31. Qi Q, You Q, Gu H, et al. Studies on the toxicity of gambogic acid in rats. *J Ethnopharmacol*. 2008;117(3):433-438.
32. Wang S, Yang Y, Wang Y, Chen M. Gambogic acid-loaded pH-sensitive mixed micelles for overcoming breast cancer resistance. *Int J Pharm*. 2015;495(2):840-848.
33. Ji Y, Shan S, He M, Chu CC. Inclusion complex from cyclodextrin-grafted hyaluronic acid and pseudo protein as biodegradable nano-delivery vehicle for gambogic acid. *Acta Biomater*. 2017;62:234-245.
34. Yan X, Yang Y, He L, Peng D, Yin D. Gambogic acid grafted low molecular weight heparin micelles for targeted treatment in a hepatocellular carcinoma model with an enhanced anti-angiogenesis effect. *Int J Pharm*. 2017;522(1-2):110-118.
35. Sercombe L, Veerati T, Moheimani F, Wu SY, Sood AK, Hua S. Advances and challenges of liposome assisted drug delivery. *Front Pharmacol*. 2015;6:286.
36. Patel NR, Pattni BS, Abouzeid AH, Torchilin VP. Nanopreparations to overcome multidrug resistance in cancer. *Adv Drug Deliv Rev*. 2013;65(13-14):1748-1762.
37. Schoellhammer CM, Blankschtein D, Langer R. Skin permeabilization for transdermal drug delivery: recent advances and future prospects. *Expert Opin Drug Deliv*. 2014;11(3):393-407.
38. Prausnitz MR, Langer R. Transdermal drug delivery. *Nat Biotechnol*. 2008;26(11):1261-1268.
39. Labala S, Mandapalli PK, Kurumaddali A, Venuganti VV. Layer-by-layer polymer coated gold nanoparticles for topical delivery of imatinib mesylate to treat melanoma. *Mol Pharm*. 2015;12(3):878-888.
40. Jiang T, Wang T, Li T, et al. Enhanced transdermal drug delivery by transfersome-embedded oligopeptide hydrogel for topical chemotherapy of melanoma. *ACS Nano*. 2018;12(10):9693-9701.
41. OECD. *Guideline for Testing of Chemicals 404. Acute Dermal Irritation/Corrosion*. Paris, France: Organization for Economic Cooperation and Development; 2015.
42. Barry BW. Novel mechanisms and devices to enable successful transdermal drug delivery. *Eur J Pharm Sci*. 2001;14(2):101-114.
43. Goodman M, Barry BW. Action of penetration enhancers on human skin as assessed by the permeation of model drugs 5-fluorouracil and estradiol. I. Infinite dose technique. *J Invest Dermatol*. 1988;91(4):323-327.
44. Williams AC, Barry BW. Penetration enhancers. *Adv Drug Deliv Rev*. 2012;64:128-137.
45. Yuan X, Capomacchia AC. Physicochemical studies of binary eutectic of ibuprofen and ketoprofen for enhanced transdermal drug delivery. *Drug Dev Ind Pharm*. 2010;36(10):1168-1176.
46. Milewski M, Stinchcomb AL. Estimation of maximum transdermal flux of nonionized xenobiotics from basic physicochemical determinants. *Mol Pharm*. 2012;9(7):2111-2120.
47. Wong TW. Electrical, magnetic, photomechanical and cavitational waves to overcome skin barrier for transdermal drug delivery. *J Control Release*. 2014;193:257-269.
48. Godin B, Touitou E. Transdermal skin delivery: predictions for humans from in vivo, ex vivo and animal models. *Adv Drug Deliv Rev*. 2007;59(11):1152-1161.
49. Zhang Y, Yang ZJ, Tan XY, Tang X, Yang ZX. Development of a more efficient albumin-based delivery system for gambogic acid with low toxicity for lung cancer therapy. *AAPS PharmSciTech*. 2017;18(6):1987-1997.
50. Menon GK, Cleary GW, Lane ME. The structure and function of the stratum corneum. *Int J Pharm*. 2012;435(1):3-9.
51. Wagner H, Kostka KH, Lehr CM, Schaefer UF. pH profiles in human skin: influence of two in vitro test systems for drug delivery testing. *Eur J Pharm Biopharm*. 2003;55(1):57-65.
52. Hikima T, Tojo K. Binding of prednisolone and its ester prodrugs in the skin. *Pharm Res (N Y)*. 1997;14(2):197-202.
53. Li JL, Xu WT, Liang YB, Wang H. The application of skin metabolomics in the context of transdermal drug delivery. *Pharmacol Rep*. 2017;69(2):252-259.
54. Xu XQ, Zhu QH. Evaluation of skin optical clearing enhancement with Azone as a penetration enhancer. *Opt Commun*. 2007;279(1):223-228.
55. Chen HL, Cai CC, Ma JY, et al. Effect of the dispersion states of azone in hydroalcoholic gels on its transdermal permeation enhancement efficacy. *J Pharm Sci*. 2018;107(7):1879-1885.
56. Tofovic SP, Jackson EK. Effects of long-term caffeine consumption on renal function in spontaneously hypertensive heart failure prone rats. *J Cardiovasc Pharmacol*. 1999;33(3):360-366.
57. Wang J, Li Z, Sun F, et al. Evaluation of dermal irritation and skin sensitization due to vitacoxib. *Toxicol Rep*. 2017;4:287-290.
58. Lulekal E, Tesfaye S, Gebrechristos S, et al. Phytochemical analysis and evaluation of skin irritation, acute and sub-acute toxicity of *Cymbopogon citratus* essential oil in mice and rabbits. *Toxicol Rep*. 2019;6:1289-1294.